Gating of *Shaker* K^+ Channels: II. The Components of Gating Currents and a Model of Channel Activation

Francisco Bezanilla,* Eduardo Perozo,‡ and Enrico Stefani§

*Department of Physiology, University of California at Los Angeles, Los Angeles, California 90024, and §Department of Physiology and Molecular Biophysics, Baylor College of Medicine, Houston, Texas 77030 USA

ABSTRACT Steady-state and kinetic properties of gating currents of the *Shaker* K^+ channels were studied in channels expressed in *Xenopus* oocytes and recorded with the cut-open oocyte voltage clamp. The charge versus potential (Q-V) curve reveals at least two components of charge, the first moving in the hyperpolarized region ($V_{1/2} = -63$ mV) and the second, with a larger apparent valence, moving in the more depolarized region ($V_{1/2} = -44$ mV). The kinetic analysis of gating currents revealed also two exponential decaying components that corresponded in their voltage dependence with the charge components described in the steady-state. The first component was found to correlate with the effects of prepulses that produce the Cole-Moore shift of the ionic and gating currents and seems to be occurring completely within closed conformations of the channel. The second component seems to be related to the events occurring between the closed states just preceding, but not including, the transition to the open state. The ON and OFF gating currents exhibit a pronounced rising phase at potentials at which the second component becomes important, and this region corresponds to the potential range where the channel opens. The results could not be explained with simple parallel models, but the data can be fitted to a sequential model that could be related to a first rearrangement of the putative four subunits in cooperative fashion, followed by a concerted charge movement that leads to the open channel. The first series of charge movements are produced by transitions between several closed states carrying less than two electronic charges per step, while a step carrying about 3.5 electronic charges can explain the second component. This step is followed by the transition to the open state carrying less than 0.5 electronic charges. This model is able to reproduce all the kinetic and steady-state properties of the gating currents and predicts many of the properties of the ionic currents.

INTRODUCTION

In voltage-dependent channels, the probability of channel opening is modulated by the membrane potential. The mechanism by which the transmembrane electric field can produce this modulation is still not understood. As predicted by Hodgkin and Huxley (1952), the coupling between channel gating and membrane voltage must involve the presence of charges or electric dipoles able to sense the potential drop across the membrane. The movement of these sensors in the membrane produce capacitive currents named gating currents (Armstrong and Bezanilla, 1973). The recordings of these gating currents are expected to reveal details of the conformational changes in the channel molecule, because their magnitude and time course are a direct expression of the change in polarization as a result of the movement of the voltage sensors.

The kinetic information gathered by electrophysiological measurements in voltage-dependent channels such as the *Shaker* K^+ channel indicate that the channel protein may dwell in several kinetic states, most of them in closed conformation, and that many of the transitions between states are governed by the membrane potential (i.e., Zagotta and Aldrich, 1990). It is then expected that every voltage-dependent transition will have a voltage sensor, and its change in polarization induced by a sudden voltage change will generate a transient current. The analysis of channel opening with macroscopic ionic currents or single channel recordings reveal details of the gating process preferentially in the neighborhood of the open state of the channel. In contrast, gating currents show details of the channel operation for all the voltage-dependent transitions, therefore it is expected to give important information about transitions between closed states. For this reason, a detailed description of the gating process requires an in depth analysis of gating currents.

In general, the net flow between two states times the charge times the fraction of the electric field constitutes the gating current I_i of that particular transition:

$$I_i = Nez_i(f_i - f_{i+1})$$

where N is the total number of channels, e is the electronic charge, i represents the index of the particular state with flow f_i to the state i+1 and reverse flow f_{i+1}, z_i is the effective valence times the fraction of the field involved in the transition between s_i and s_{i+1}. Therefore the observed gating current will be sum of all these individual currents over all possible transitions:

$$I = \sum I_i$$

It is clear then that the kinetics of the macroscopic gating current will reflect the contribution of all the individual transitions weighted according to the initial conditions and relative population of each of the states. Because there is a large

Received for publication 19 August 1993 and in final form 10 December 1993.

Address reprint requests to Francisco Bezanilla, Department of Physiology, UCLA School of Medicine, 405 Hilgard Ave., Los Angeles, CA 90024.

‡Present address: Centro de Biofisica y Bioquimica, Instituto Venezolano de Investigaciones Cientificas, Apartado 21827, Caracas 1020A, Venezuela.

0006-3495/94/04/1011/11 $2.00

number of states with different voltage-dependent transition probabilities, it is expected that the kinetic schemes describing this behavior will be quite complex. Nevertheless, in specific kinetic schemes it may be extremely simple: such is the case of independent identical gating particles which corresponds to the Hodgkin and Huxley-type of models (Hodgkin and Huxley, 1952).

Gating currents from Shaker K^+ channels have been recorded by several laboratories using different techniques, providing several new details of the channel's voltage dependence useful in the correlation between structure and function (Stühmer et al., 1991; Bezanilla et al., 1991; Perozo et al., 1992; Schoppa et al., 1992). We report in this paper a detailed analysis of the gating current kinetics of the noninactivating (Hoshi et al., 1990; Zagotta et al., 1990), nonconducting mutant W434F of the *Shaker* H4-IR channel (*Sh*H4-IR-W434F (Perozo et al., 1993)). This channel is expressed in high densities in *Xenopus* oocytes and studied with high resolution voltage clamp using the cut-open oocyte technique (Stefani et al., 1994; Taglialatela et al., 1992). The results show that the gating charge has at least two components with different voltage dependencies and that the gating currents show complex kinetic behavior depending on voltage and initial conditions. These features allowed us to test and evaluate different types of models. We have confirmed that a model of several independent identical subunits making first order transitions is incompatible with the results and that a class of parallel models is not compatible either. Some types of sequential models can account for most of the results, and we present an example of a kinetic model which predicts macroscopic ionic and gating currents under a variety of conditions.

MATERIALS AND METHODS

Most of the experiments were done with the noninactivating (Zagotta et al., 1990) nonconducting mutant W434F of the H4-IR variety *of Shaker* K^+ channel (*Sh*H4-IR-W434F (Perozo et al., 1993)) expressed in *Xenopus* oocytes and studied with the cut-open oocyte technique. Macroscopic ionic currents were studied with the H4-IR mutant of *Shaker* and minimizing series resistance errors as described in the previous paper. For details of the techniques see Materials and Methods of the previous paper (Stefani et al., 1994). External solution was NaMESCa2 and internal KGLU EGTA1 in saponin-open oocytes with series resistance compensation as discussed in the previous paper (Stefani et al., 1994).

Kinetic models were generated and evaluated using ScoP, a simulation and model generation environment (Simulation Resources, Barrien Springs, MI) and the fits were done directly to the parameters of the model using ScoPfit. A set of 12 gating current traces to different depolarizations including data during and after the pulse, was used to fit to the numerical solution of kinetic models. The rate constants were assumed to be of the form

$$\alpha = \alpha_0 \exp[zxeV/kT]$$

for the forward rates α and

$$\beta = \beta_0 \exp[-z(1 - x)eV/kT]$$

for the backward rates β, where α_0 and β_0 are the rates at 0 mV, z is the valence of the charge moving in the entire field, x is the fraction of the field where the peak of the barrier is located, V is the membrane potential, e is the electronic charge (1.6×10^{-19} coul), and k and T are the Boltzmann constant and absolute temperature, respectively. Initial conditions were also fit to the data and the adjustable parameters were the valence, fraction of the field and value of the rate at zero potential for each of the rate constants.

RESULTS

General kinetic features

A set of gating current records is shown in Fig. 1, where the initial time of each sweep has been displaced to improve visibility of the kinetic features during and after the depolarization. These currents were recorded from a holding potential of −90 mV to the indicated potentials without the use of subtracting pulses and using analog subtraction to eliminate the linear capacity transient. The analog subtraction was applied by compensating the capacitive transient while holding the membrane potential at 0 mV, a potential at which the charge movement has no voltage dependence. The gating currents exhibit a rising phase that is barely visible for small pulses but becomes quite pronounced at large depolarizations. This behavior is similar to that observed previously in gating current records obtained using subtracting pulses (Bezanilla et al., 1991; Perozo et al., 1992).

The decay phase of the gating current during the pulse (ON phase) is fast for small depolarizations, resembling a single exponential process. However, at intermediate depolarizations a second slower component appears that tends to grow as the depolarization increases. Both components appear to merge in one fast decay phase at larger depolarizations.

At the end of the pulse, returning to −90 mV, the OFF gating currents show additional kinetic features (Fig. 1). For small pulse depolarizations, the off gating current is fast and without an appreciable rising phase. The return from larger depolarizations exhibits a fast component followed by a slower decay and for even larger pulses, the OFF gating currents show a rising phase followed by a very slow decay that does not change for pulses larger than about −20 mV.

The steady-state voltage dependence of the gating charge

To obtain the voltage dependence of the charge transfer, we have integrated gating current traces for pulses up to 120 ms long (such as the ones shown in Fig. 1) for a series of pulses ranging from −150 to +20 mV in 2-mV increments (Fig. 2 *a*). It is apparent that the charge distribution is

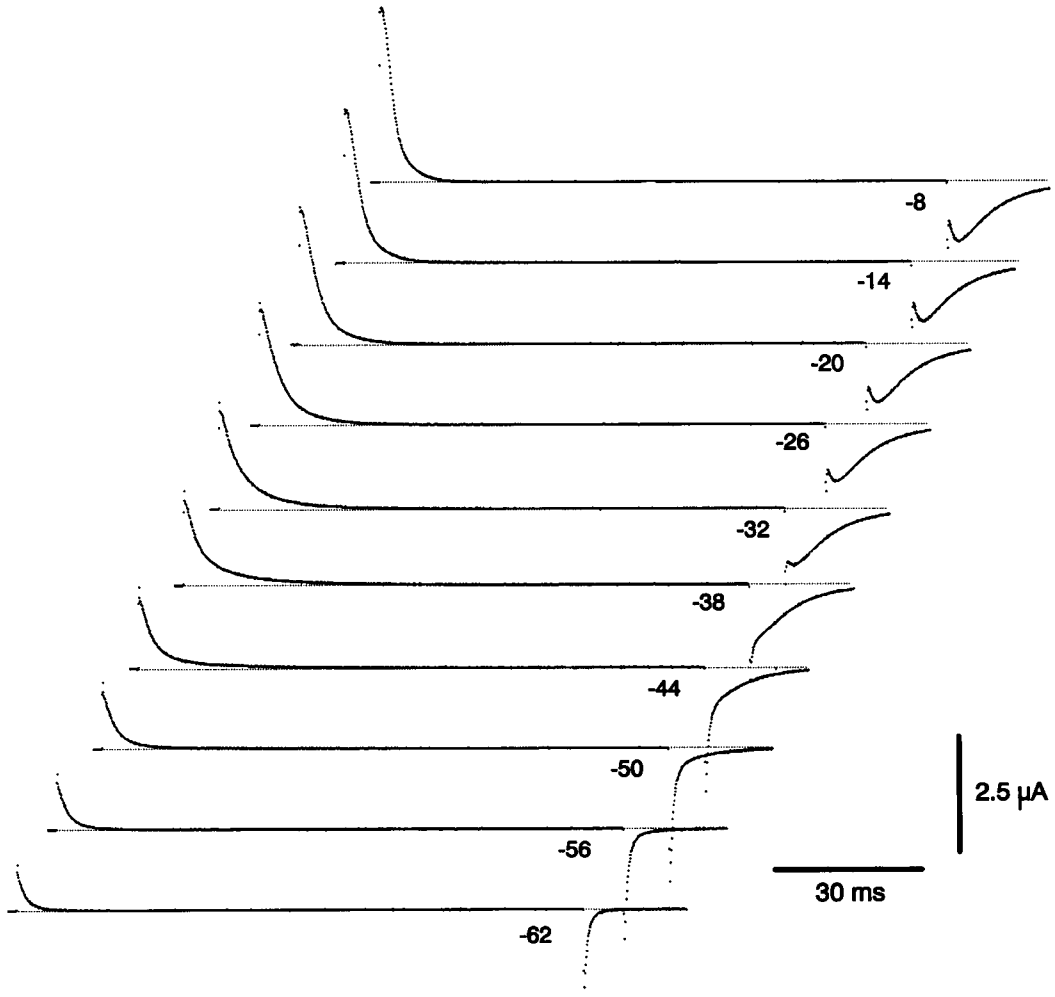

FIGURE 1 Experimental recordings of gating currents. The holding potential was −90 mV, and the pulses were 120 ms long to the indicated potentials. Traces have been shifted to the right to prevent overlap that masks significant kinetic features. No P/4 subtraction was used, instead the linear capacity transient recorded at 0 mV was compensated with an analog waveform consisting of three exponential components. Temperature 18.5°C.

asymmetrical, having a shallower slope at negative potentials than at the positive saturating potentials. This can be easily seen when comparing the experimental points with a fitted single Boltzmann distribution (thin line) that fails to fit adequately in both ends of the curve. By contrast, when the charge is fitted to two Boltzmann distributions, the agreement with the data is excellent, as shown by the close correspondence between the continuous thick line and the data points in Fig. 2 *a*. The two Boltzmann components have been plotted in the same figure and labeled as Q_1 and Q_2. The fitted values for the equivalent valences are 2.3*e* for Q_1 and 4.86*e* for Q_2, while the midpoints of the curves are −64 mV for Q_1 and −46 mV for Q_2, showing that Q_1 develops at more negative potentials, carries less charge and has less voltage dependence than Q_2. Although it is tempting to conclude from this analysis that there are two separate charge systems in the Shaker K^+ channel gating current, the data can be fitted as well by a sequential three state model. The fitted curve for the sequential model is also superimposed in the data of Fig. 2 *a*, and it is indistinguishable from the parallel model. The individual components of the sequential model are slightly different and are labelled Q'_1 and Q'_2 in Fig. 2 *a* with values for valence and midpoints of 2.17*e* and −61.4 mV for Q'_1 and 4.44*e* and −46.3 mV for Q'_2. We will see below that kinetic analysis of the charge movements will indicate that it is more likely that the two components are not completely independent of each other. Table 1 lists the values of the valences and midpoints of the double Boltzmann fits for several experiments.

The significance of the two components of charge can be dissected by double pulse experiments such as the protocol first tested by Cole and Moore (1960). Fig. 3 *a* shows gating currents recorded for a pulse to 0 mV from a set of different initial prepulses 5 ms in duration. The time course of the gating current is dramatically affected by the magnitude of the prepulse even though the pulse potential is the same. When the prepulse is more negative than −80 mV the current shows a pronounced rising phase that is not observed for prepulses near −42 mV. In addition, the decay phase of the current is delayed for more negative prepulses increasing the charge moved during the gating current transient. The

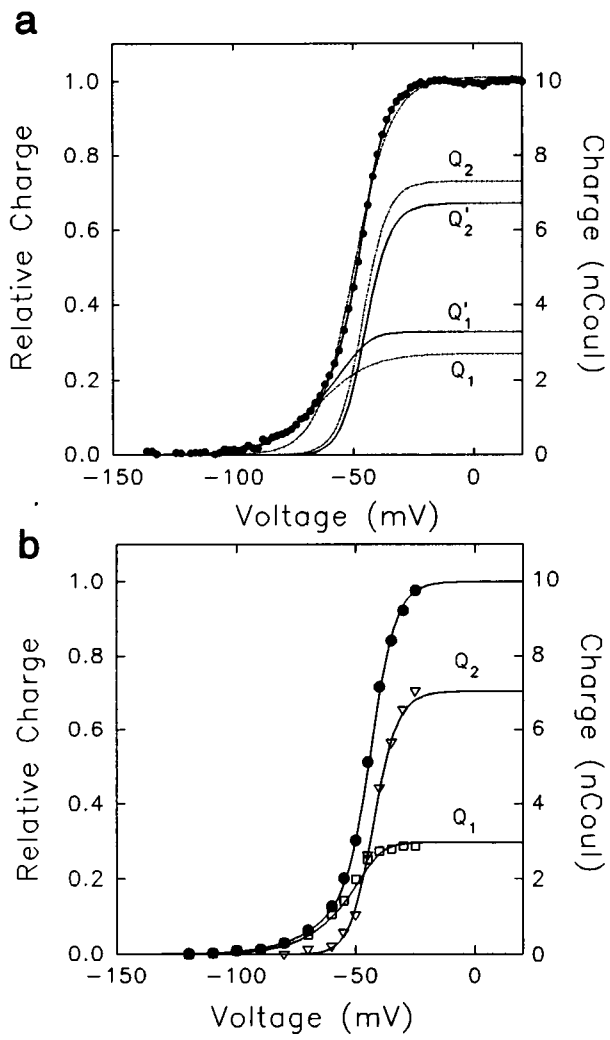

FIGURE 2 Distribution of gating charge with membrane potential. (*a*) The charge was obtained as the time integral of the gating current. The *Q-V* curve was fitted poorly by a simple Boltzmann distribution of the form,

$$q(V) = \frac{q_{max}}{1 + \exp[-ze(V - V_1)/kT]}$$

(the *dotted line* that deviates from the experimental points) with $z = 3.2$ and $V_1 = -49.4$, but it can be fitted very well by *a*, the sum of two Boltzmann distributions,

$$q(V) = \frac{q_1}{1 + \exp[-z_1e(V - V_1)/kT]} + \frac{q_2}{1 + \exp[-z_2e(V - V_2)/kT]}$$

(the *line* that follows the points). In the same figure the two Boltzmann components (Q_1 and Q_2) have been plotted as the continuous lines without experimental points. Fitted parameters were $z_1 = 2.3$, $V_1 = -64.9$ mV, $z_2 = 4.86$ and $V_2 = -46$ mV. A fit to a sequential three state model is also shown and the line is indistinguishable from the fit to the two independent Boltzmann distributions. The individual components of this fit are plotted as dotted lines and labelled as Q_1' and Q_2' with parameters $z_1' = 2.17$, $z_2' = 4.44$, $V_1' = -61.4$ and $V_2' = -46.3$ mV. (*b*) The components of the *Q-V* curve obtained as the integral of two exponential decay functions obtained as the integral of two exponential decay functions fitted to the gating currents. The parameters fitted were: $z_1 = 2.1$, $V_1 = -52$ mV, $z_2 = 4.3$ and $V_2 = -45$ mV. For details see text.

magnitude of the ON charge during the test pulse as a function of the prepulse potential V_p is defined as $q(V_p)$, and it is plotted in Fig. 3 *b* as the solid triangles. We can estimate

TABLE 1 The parameters of two Boltzmann distributions fitted to several experiments

Experiment	V_1 (mV)	z_1	V_2 (mV)	z_2
1	−65	2.01	−44	5.63
2	−56	3.12	−42	4.91
3	−70	2.33	−43	5.40
4	−61	2.17	−46	4.43
5	−64	2.38	−46	4.86
Mean ± SD	−63.2 ± 5.1	2.4 ± 0.42	−44.2 ± 1.7	5.04 ± 0.47

the dependence of the charge transferred upon initial conditions by computing

$$\Delta Q = q(-120) - q(V_p)$$

which is plotted as closed squares in Fig. 3 *b*. In the same figure, the closed circles represent the charge transferred during the test pulse as a function of the test pulse amplitude (regular *Q-V* curve). It can be seen that the charge elicited by the prepulses from −120 to −42 mV nicely matches the total charge in this voltage range. As this charge is mostly carried by Q_1, it indicates that Q_1 is responsible for most of the Cole-Moore shift. A prepulse of only 5-ms duration is enough to move all the charge at potentials more negative than −52 mV, showing that the kinetics of Q_1 is fast as compared to Q_2 (see below). We have shown in the accompanying paper (Stefani et al., 1994) that the shift of the decay phase of the gating current with the negative prepulse is paralleled by the classical Cole-Moore shift of the ionic currents, therefore we can conclude that Q_1 corresponds to the charge that moves in transitions between closed states of the channel and that it is not directly associated with the actual opening of the channel.

Kinetic separation of the charge components of the ON gating current

Inspection of Fig. 1 reveals that at small depolarizations the currents decay very quickly, at intermediate depolarizations (to about −40 mV) there are clearly two decaying phases and at large depolarizations both decaying phases seem to merge in a single faster decay. To quantify these changes and in an attempt to separate kinetic components in the gating currents, the currents were fitted to a sum of two decaying exponentials. The fits were done to records obtained for pulses of long duration (100 or 120 ms). This is to improve the resolution of the slow component at negative potentials where it is slow enough that for shorter pulses it could be confused with a raised or sloping baseline. In some sets of records the fits to the experimental points were performed about 300 μs after the pulse to exclude the rising phase, and in other sets the rising phase was included but a third rising exponential was also fitted. In both cases the fitted decaying exponentials were very similar (not shown).

An example of these fits is shown in Fig. 4. for some representative depolarizations. The left panel shows data points from the original traces with the fitted sum of two exponentials (*continuous line*). The right panel shows the

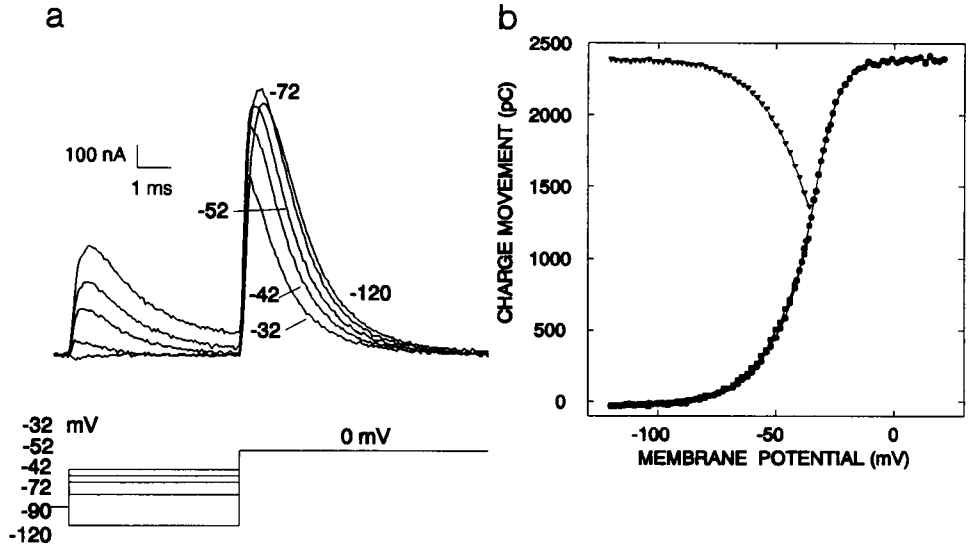

FIGURE 3 Cole-Moore shift of gating currents. (*a*) Superimposed gating current records for a pulse to 0 mV from different prepulses to −120, −72, −52, −42, and −32 mV lasting 5 ms. (*b*) The *Q-V* curve as determined from the integral of gating currents (●); the charge elicited during the test pulse as a function of the prepulse (▼) and the extra charge elicited during the test pulse as a function of the magnitude of the prepulse (■). Temperature, 22°C. For details, see text.

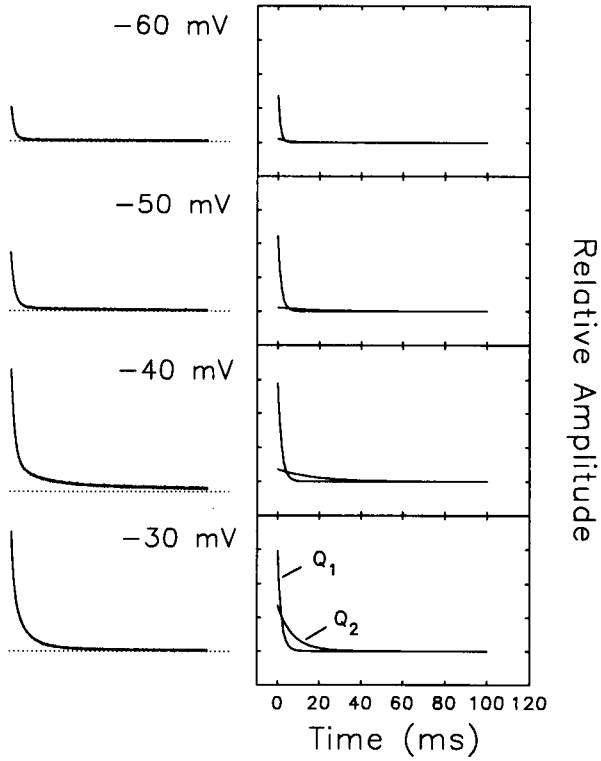

FIGURE 4 (*Left panel*) Gating currents for the depolarizations as indicated with superimposed fitting of two exponential decaying functions. (*Right panel*) Plot of the time course of the two exponential components used to fit the gating currents in part *a* for the corresponding depolarizations. Temperature, 20°C.

two exponential components independently. The initial amplitude of the Q_1 component increases steeply between −60 and −40 mV, but it does not increase much more between −40 and −30 mV. In addition, the time constant decreases with depolarization but it tends to saturate at about −30 mV as is shown in the lower panel of Fig. 5. On the other hand, the magnitude of Q_2 increases continuously in the range from −60 to −30 mV, while its time constant first increases and then decreases with depolarization, as shown in the upper panel of Fig. 5. Beyond −20 mV the two exponential components tend to merge in a single exponential, and it is no longer possible to separate them kinetically. The relative charge carried by each exponential components can be estimated analytically by multiplying the fitted amplitude coefficient times the time constant. This was done for all the fitted potentials, and it is plotted in Fig. 2 *b*. The striking similarity between the steady-state separation shown in Fig. 2 *a* and the kinetic separation shown in Fig. 2 *b* supports the idea of two gating components which differ in their voltage dependencies and their relative position in the voltage axis.

As the two components activate in different voltage regions, it should be possible to isolate Q_2 by pulsing the membrane to a potential where most of the Q_1 has already moved. Fig. 6. shows the results of such experiment. The membrane was pulsed to −60 mV for 120 ms before the test pulse was applied. The gating current during the test pulse was fitted to two exponentials, and the two components of charge were estimated by the product of the coefficient and the time constant, as explained above. Fig. 6 *a* shows the charge carried by the two components, indicating that the proportion between the Q_1 (*squares*) and Q_2 (*circles*) is favored to the Q_2, as compared to the case where the prepulse potential is −90 mV, shown in Fig. 6 *b*. This result confirms the idea that a large fraction of Q_1 has moved at −60 mV, therefore pulsing from this potential the gating current is preferentially carrying the Q_2 component.

Separation of the charge components at the *Off* gating current

The kinetics of the charge return is a complex function of the pulse potential as can be seen in Fig. 1. For small depolarizations (pulses to −60 mV) the charge returns very quickly, for larger depolarizations the OFF gating currents has a fast component followed by a smaller slower component. At

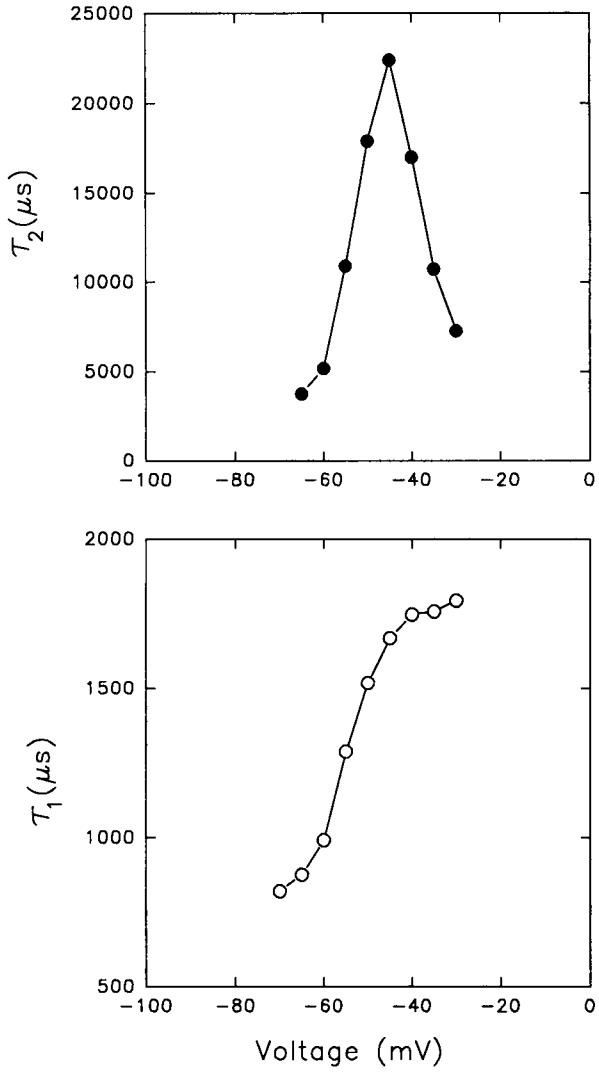

FIGURE 5 Time constants of the exponential components. (*a*) Voltage dependence of the time constant of the Q_2 component. (*b*) Voltage dependence of the time constant of the Q_1 component. Temperature, 20°C.

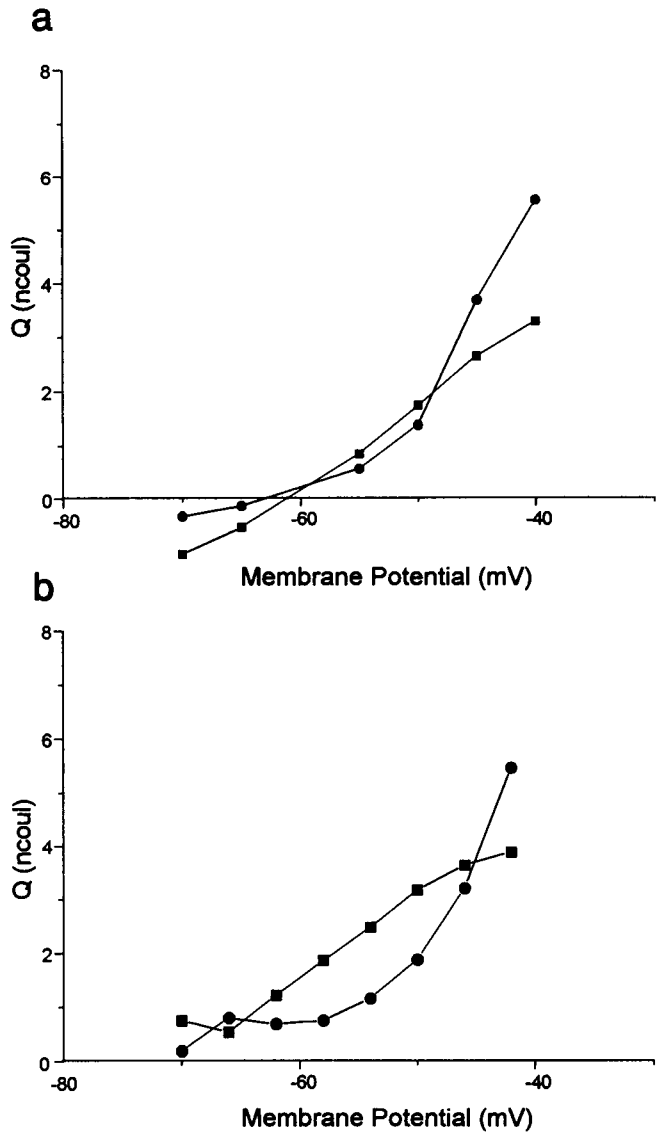

FIGURE 6 The two charge components calculated from the fitted exponential decays as a function of initial conditions. The squares represent the area of the fitted Q_1 component, and the circles correspond to the area of the fitted Q_2 component. Holding potential was −90 mV. (*a*) Prepulse to −60 mV for 120 ms. (*b*) No prepulse. Temperature, 18.5°C.

larger depolarizations the actual peak value of the OFF gating current becomes smaller, exhibits a rising phase and a very slow decay. These OFF components can be traced to the corresponding ON components discussed above, because the fast OFF occurs only when the Q_1 has developed during the pulse and the slow OFF is observed at potentials where the Q_2 has appeared during the ON gating current. It must be noted, however, that these two components do not appear as independent charge movements. If that were the case, it would be expected that the OFF gating current should show a monotonic increase in its amplitude with pulse amplitude, maintaining the two exponential decaying components in proportion of their appearance in the ON phase.

A confirmation that the components in the OFF gating current are related to the ON components is shown in Fig. 7. Traces of gating current with different pulse durations elicited by pulsing to −35 mV and returning to −90 mV are superimposed in Fig. 7 *a*. It is evident that the OFF gating current becomes progressively slower with pulse duration, but it does so by the appearance of a second exponential component in the OFF that becomes larger with pulse duration at the expense of a decrease of the amplitude of the fast component, showing again that the two components do not simply add independently. It is also clear from Fig. 7 *a* that the appearance of the slow OFF component follows the time course of the slow component of the ON gating current. At −35 mV the gating charge is not fully developed, and the OFF gating does not show a clear rising phase even for long pulses. When the depolarization is to 0 mV (a potential at which all the charge has moved), the second component develops earlier in the pulse, and the rising phase of the OFF is clearly observed for durations longer than about 7 ms (Fig. 7 *b*). These results indicate that the appearance of the

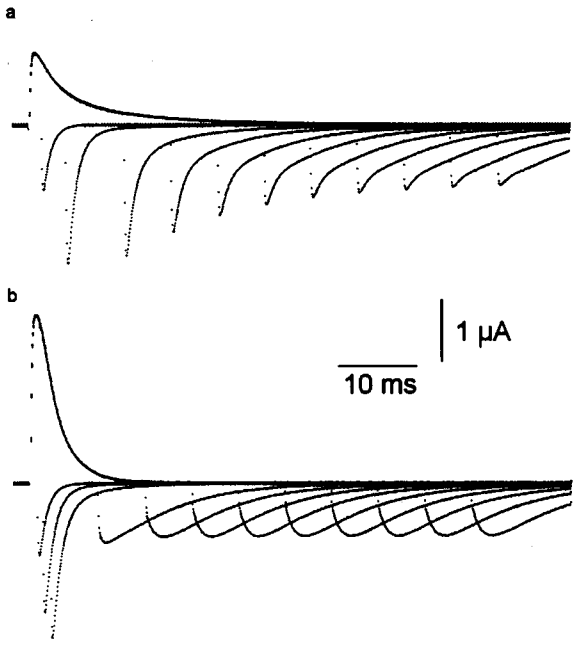

FIGURE 7 The OFF gating current as a function of pulse duration. (*a*) Pulse from −90 mV to −35 mV and returning to −90 mV for durations of 1.2, 3.8, 10, 15, 20, 25, 30, 35, 40, 45, and 50 ms. (*b*) Pulse from −90 mV to 0 mV and returning to −90 mV for pulse durations of 0.6, 1.2, 2, 7, 12, 17, 22, 27, 32, 37, 42, and 47 ms. Unsubtracted records. Temperature, 18.5°C.

slow component in the OFF gating current requires the movement of the Q_2 during the pulse.

The pulse protocol shown in Fig. 8 demonstrates the connection between the two charge components. The first pulse develops a fraction of the charge depending on the amplitude of the depolarization, then there is a variable recovery interval at −90 mV before the third test pulse to 0 mV is applied. In Fig. 8 *b* the first pulse is to −60 mV and 50-ms duration, and it can be observed that the gating current during the third pulse is always fully developed regardless of the duration of the second pulse, indicating that the charge returns in a very short time after the first pulse (less than 700 μs) and it is all available to move for the third pulse. In Fig. 8 *c*, the amplitude of the first pulse is −40 mV and in this case a recovery of 700 μs makes only one-fourth of all the charge available for the third pulse. Full recovery can only be obtained with a period of about 20 ms at −90 mV. In Fig. 8 *d* the first pulse is 0 mV, and in this case 700 μs recovers less than 5% of the charge and again a full recovery is obtained with more than 20 ms at −90 mV. These results indicate that the two charge components do not move independently. A pulse to −60 mV moves mainly the Q_1 component and it is easily reversible. On the other hand, a pulse to −40 mV or to 0 mV moves more of Q_2 and none of the charge comes back immediately. This shows that the more complete is the transfer of Q_2, the less mobile is Q_1 as if the two charge movements are somehow interdependent.

The reactivation experiment, initially used by Oxford (1981) for sodium ionic currents, also indicates that the last step is not rate limiting. One can imagine that after the charge has moved with the first pulse, a brief return to −90 mV will only populate states very close to the open state and the third pulse will be an indication of the charge movement only between these last states. If the last step were a rate-limiting step, it is expected that the main exponential decay of the gating current during the third pulse should be independent of the recovery interval. Inspection of Fig. 8 *d* shows that the

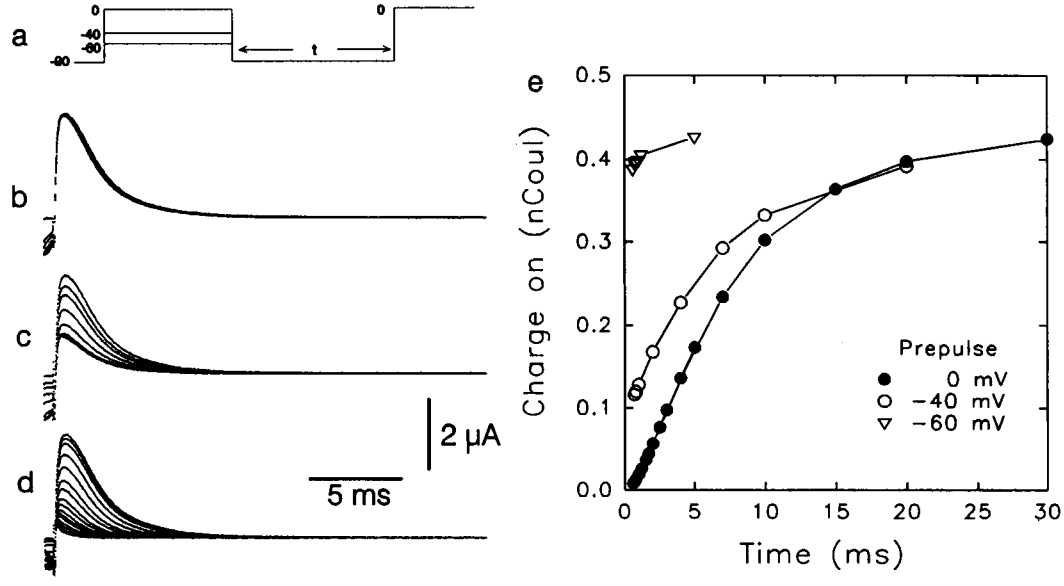

FIGURE 8 Reactivation of gating currents after a variable recovery interval for three different values of activating pulses. (*a*) Pulse protocol. The first pulse took the membrane potential to −60, −40, or 0 mV for 50 ms, then a variable recovery interval of *t* ms at −90 mV was followed by a test pulse to 0 mV, and all the recordings shown are for this last pulse. (*b*) Superimposed traces for a first pulse to −60 mV. (*c*) Traces for a first pulse to −40 mV. (*d*) Traces for a first pulse to 0 mV. (*e*) The charge, evaluated as the integral of the gating current during the test pulse, for different values of the first pulse, as indicated, as a function of the recovery period at −90 mV. Unsubtracted records. Temperature, 18.5°C.

time course of the gating current for short recovery is faster than for long recoveries indicating that the last step is not rate-limiting but in fact relatively fast. The exact relation of rates among the states cannot be stated quantitatively unless the data are fitted to a model.

The voltage dependence of charge return

The kinetics of the OFF gating current is not only dependent on the potential during the pulse but also is very voltage-dependent on the potential after the pulse. Fig. 9 *a* shows a series of OFF gating current traces for a 120-ms pulse to 30 mV and returning to a range of potentials. In all cases a rising phase is present but the decaying phase becomes faster as the potential is made more negative. The decaying phase can be fitted with two exponential components, and their voltage dependence is shown in Fig. 9 *b*. The predominant (faster) component (more than 90%) is almost exponentially dependent on voltage showing a slight tendency to saturate at potentials near −150 mV.

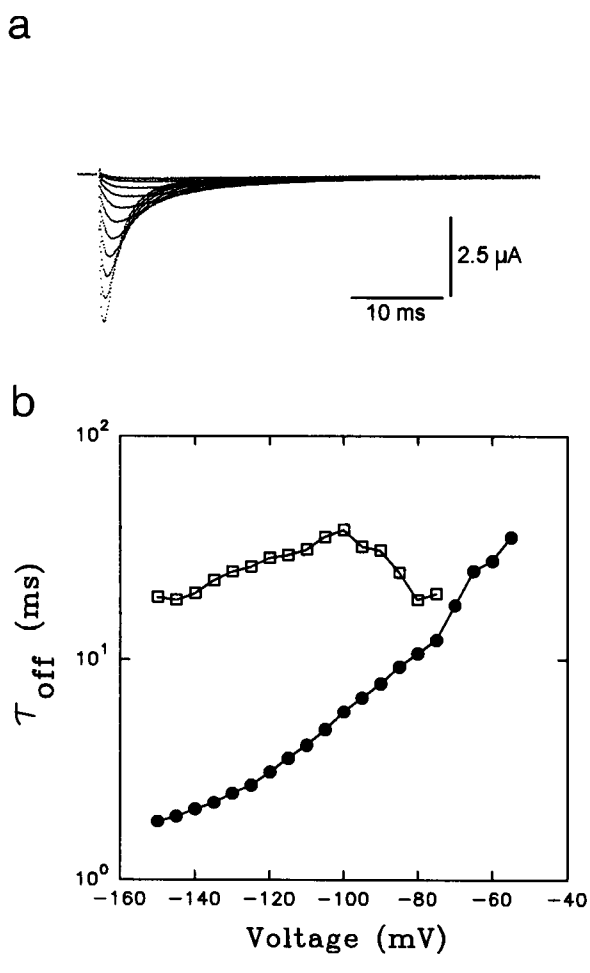

FIGURE 9 The tail kinetics is dependent on the membrane potential. (*a*) Superimposed traces returning from from +30 mV to potentials ranging from −150 (the largest current) to −50 mV (the smallest current). (*b*) Time constants of the decaying phase of the gating current tails as a function of membrane potential during the tail. Temperature, 18.5°C.

DISCUSSION

The results presented here are of interest, because they show that gating currents exhibit complex kinetic features that should facilitate the discrimination among different classes of kinetic models. Simple models, such as Hodgkin and Huxley-type, where several independent identical subunits, each moving between two states, predict that the gating current would exhibit a simple relaxation and the *Q-V* curve should be a simple Boltzmann distribution. The results of this paper have shown that in the nonconducting mutant of the Shaker *Sh*H4-IR-W434F the gating current is made of two distinct kinetic components that account for two clearly different regions in the *Q-V* curve, invalidating this type of model.

We have considered two general classes of models in an attempt to explain the gating current data quantitatively. The first type could be called a parallel model (Spires and Begenisich, 1989) in which two separate charge systems that respond to the field make several transitions independent of each other. Opening of the channel (the framed states in Fig. 10 *a*) occurs if and only if both systems have reached to the rightmost closed state. One charge system moves at more negative potentials than the other (Q_1) and carries less charge in all its transitions making it less steep with voltage than Q_2. The most likely stoichiometry of the channel is a homo-tetramer (MacKinnon, 1991), therefore when we assume two independent charge systems, each component is contributed by all four subunits, either independently or in cooperation but we still assume that there is no interaction between the two charge systems. In this simple way, this type of model is not consistent with the data because we have shown that the return of Q_1 is dependent on Q_2. To account for this result, the obvious modification of the parallel model is to assume that the two charges move independently in the ON phase, which occurs when starting from a negative holding potential and pulsing to a more depolarized potential, but when both charges have moved, they interact presumably

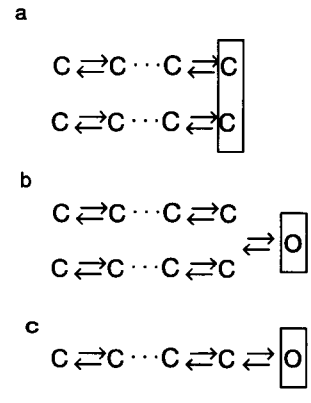

FIGURE 10 Kinetic models explored to account for the gating current data. (*a*) A parallel model with two components; the frame represents the open state which only occurs if the upper and lower C states in the frame are populated simultaneously. (*b*) Two parallel components that interact to open the channel (framed state) through one more reaction step. (*c*) A sequential model that leads to the open state (*framed state*).

leading to channel opening (see Fig. 10 *b*). This type of parallel model would explain the kinetics of the gating current tail because for small depolarizations only Q_1 has moved and it cannot interact with Q_2, therefore upon repolarization it should return quickly. On the other hand for large depolarizations, both charges have moved and they will not return independently upon repolarization until they dissociate. This model, however, does not account for the saturation of the initial amplitude of the current of the of Q_1 component seen between −40 and −30 mV (see Fig. 4, *right panel*), because during the ON phase the initial amplitude of both exponential components should increase independently. We have fitted our data to this type of model and a good agreement can be obtained for small depolarizations, but at large depolarizations, the fitted current tends to be larger, as expected from the fact that the fitted fast component keeps increasing with depolarization.

The second class of models considered is the sequential type (FitzHugh, 1965; Armstrong and Bezanilla, 1977; Armstrong and Gilly, 1979; Zagotta and Aldrich, 1990; Vandenberg and Bezanilla, 1991) where all the transitions, fast or slow, are concatenated in a linear scheme (see Fig. 10 *c*). There is evidence that this type of model accounts for many of the properties of Shaker K^+ channel single and macroscopic currents (Zagotta and Aldrich, 1990) and gating currents, in particular the Cole-Moore shift (Perozo et al., 1992). In addition, sequential models have been successful in accounting simultaneously for macroscopic currents, gating currents, and single channel data for sodium currents in the same preparation (Vandenberg and Bezanilla, 1991).

In building a kinetic model we have tried to keep it simple, while at the same time relating the kinetic steps to the putative structure of the Shaker K^+ channel. Given that the channel is made of four identical subunits (MacKinnon 1991) one would like to build this symmetry in the final kinetic model, but there are several practical problems that limit this approach. For example, the case already discarded of four independent identical subunits is easily tractable, because it generates 16 states that can be simplified to a sequential scheme with only five states with fixed ratios between the rate constants. The first generalization of this model is to assume interaction between the subunits which still maintains the same number of states but allows different relations between the rates (Vandenberg and Bezanilla, 1991). Interaction has been claimed to be important in accounting for the gating current rising phase (Perozo et al., 1992), and it has been the conclusion of the work of Tytgat et al. (1992) using channel constructs with different mutations in each one of the concatenated subunits. The model of Perozo et al. (1992) accounts for the ON rising phase and Cole-Moore shift of the gating currents, but it does not account for the gating current tails and it fails to give enough delay to the ionic currents turn-on. The second generalization of this model is to assume that each subunit may undergo more than one transition. For example, if each subunit has three states then the total number of states becomes 81 and it is not reducible to a linear sequential model, even if there are no interactions between subunits. The complexity of this type of models makes it futile to fit it to the experimental data because the large number of parameters involved cannot be estimated with any reliability. We have then arrived at a compromise between the pure kinetic model and the pure physical model by proposing a sequential model that accounts for the gating current data but it is not overly complicated and at the same time it may be interpreted on the basis of the subunit structure of the channel.

A model for gating currents in *Shaker* K^+ channel

The kinetic features of the gating current described in the results section are not easily described with simple sequential models. We must first account for two components in the ON gating current with different voltage dependencies. These features can be reproduced by a sequential model with several closed states where the transitions between initial states are fast and occur at more negative potentials than the subsequent transitions which are slower and occur at more positive potentials. This is the basic logic used in building the model shown in Table 2 along with its fitted parameters. Second, we must account for the complex tail kinetics which is fast for small depolarizations but slow at large depolarizations. This model accounts for this behavior because small depolarizations will only populate the initial closed states that can return quickly upon repolarization. However for larger pulses, the states closer to the open state get populated and the return is slowed down. In building this model we first used four transitions as a simple initial model and found that it was unable to reproduce the tails and the ON kinetics simultaneously. Insertion of more intermediate states between the states responsible for the Cole-Moore shift and the states responsible for the opening of the conductance dramatically improved the fit of the ON and OFF gating currents. This would be expected if we had added more parameters, but in fact the addition of states was done by duplicating transitions, consequently, keeping the number of parameters constant. The fitted data set contained depolarizations ranging from −66 to −18 mV including the ON and the OFF gating current without including ionic current. The initial conditions

TABLE 2 The kinetic model and the values of the fitted parameters

$$C_0 \underset{\beta_0}{\overset{\alpha_0}{\rightleftharpoons}} C_1 \underset{\beta_1}{\overset{\alpha_1}{\rightleftharpoons}} C_{11} \underset{\beta_1}{\overset{\alpha_1}{\rightleftharpoons}} C_{12} \underset{\beta_1}{\overset{\alpha_1}{\rightleftharpoons}} C_2 \underset{\beta_2}{\overset{\alpha_2}{\rightleftharpoons}} C_3 \underset{\beta_3}{\overset{\alpha_3}{\rightleftharpoons}} C_4 \underset{\beta_4}{\overset{\alpha_4}{\rightleftharpoons}} O$$

i	z_i	x_i	α_{0i} (ms^{-1})	β_{0i} (ms^{-1})
0	1.81	0.24	1.55	0.03
1	1.24	0.8	4.88	0.45
2	0.89	0.75	0.9	0.8
3	3.5	0.81	50.0	0.018
4	0.35	0.3	10	7

were also fitted, because we did not know a priori the distribution of the channel in the different states at the holding potential. Fig. 11 shows the predictions from this model for pulses of different amplitudes, durations, and for the voltage dependencies of the charge and conductance. The

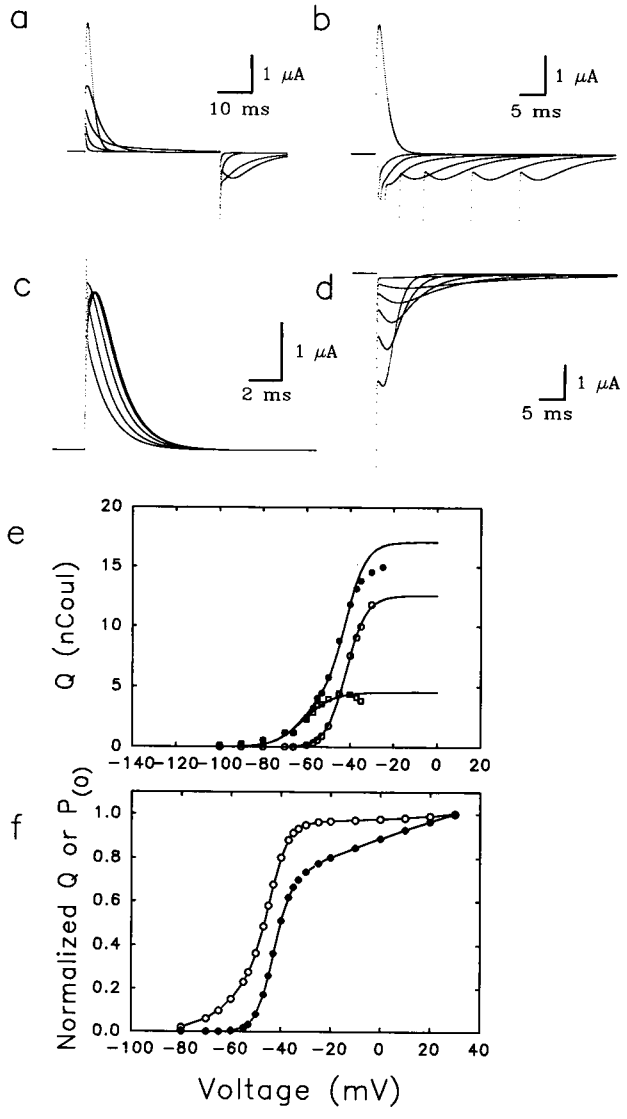

FIGURE 11 Predictions of the sequential model presented in the Discussion section. (*a*) Gating currents for different depolarizations ranging from −80 mV to 0 mV in increments of 20 mV. (*b*) The development of the tail as a function of pulse duration for a pulse to 0 mV and durations of 0.5, 1, 2, 5, 10, 20, and 30 ms, returning to −90 mV. (*c*) Cole-Moore shift of the gating currents with holding potential of −140, −120, −80, −60, −50, and −45 mV and a test pulse to 0 mV. (*d*) The voltage dependence of the gating current tail for a pulse of 0 mV and returning to −140, −120, −100, −80, −60, and −40 mV. (*e*) The separation of the kinetic components. The simulated gating currents were fitted to three exponential decaying functions and the area under the two fast functions (□) and the area under the slow function (○) are plotted versus the depolarization. The parameters for the slow component were $z = 5.38$ and $V = -41.7$ mV and for the fast component the parameters were $z = 3.36$ and $V = -60$ mV. The total area is plotted as closed circles. (*f*) The voltage dependence of the charge (Q) and the fraction of open channels ($P_{(0)}$). The $P_{(0)}$ has been normalized to the value at +30 mV.

plot in Fig. 11 *a* is the actual fit to the data. The plots in Fig. 11, *b*, *c*, and *d*, are computed with the model using the fitted parameters of Fig. 11 *a*. This model is able to generate all the kinetic and steady-state properties of *Shaker* K^+ channel gating currents.

The parameters found by the fitting routine may not be considered unique because we could not insure a global minimum. This result falls short of a unique model for gating currents of Shaker K^+ channels, nevertheless it is very useful because it allows predictions that can be tested experimentally for both gating, ionic current, and single channel fluctuations. Recent results using analysis of gating current fluctuations (Sigg et al., 1994) show consistently that one of the steps of the activation sequence carries a large charge (ca. 2.4 e^- charges) and preceding steps have smaller elementary charge. Predictions of the present model are in qualitative agreement with the time course of the mean and variance of the gating current (Sigg et al., 1994). In addition, the computation of the steady-state conductance could be also considered a prediction, because no ionic current information was included in the data set. Thus, it is striking to see that the predicted $P_{(0)}$-V curve shown in Fig. 11 *f* is similar to the G-V curve shown in Fig. 10 of the previous paper (Stefani et al., 1994). The predicted G-V curve shows the creep with potential observed between −10 and +30 mV which is the result of the small charge in the transition leading to the open state. The connection between the open state and the last closed state is probably the least reliable in this model and an alternative arrangement could be that the state C_4 becomes the open state and another closed state comes out from this new O state as a "flickery state." We believe that a simultaneous fitting of gating, ionic currents, gating fluctuations, and single channel currents should help in resolving this issue and at the same time should help to constrain the parameters even more and perhaps make the fit unique. This will require the gathering of the information from the same membrane, using impermeant ions, and blockers.

It is possible to correlate the model presented in Table 2 with a physical interpretation of the states. We may consider that the first four transitions correspond to the initial charge translocation of the four subunits which exhibit cooperativity. This process occurs entirely between closed states, and it is responsible for the Cole-Moore shift. The next two transitions would occur after the four subunits have relocated and would constitute a rearrangement that finally leads to opening of the channel represented by the last transition that is fast and does not carry too much charge. Upon repolarization, the return from the open to the first closed state is fast, producing the main deactivation rate of the ionic current (see Figs. 8 and 9, preceding paper (Stefani et al., 1994)), and it corresponds to the obliteration of the ionic pathway. During repolarization, the next transition is in fact rate-limiting (see Table 2) and produces the slow falling phase of the gating current and the slower component of deactivation seen in the ionic current tails (Fig. 9 in Stefani et al. (1994)). The correspondence

of the slow gating current decay and the slow component of the ionic current has been presented before (Bezanilla et al., 1991).

The double exponential decay of the ionic current tail deserves further discussion. This has usually been interpreted as the deactivation of two types of channels or the presence of two open states. Neither of these interpretations seems to be relevant here, because this is a cloned channel of one type and previous measurements of single channels have not revealed two open states. A simple explanation for a double exponential ionic current tail resides in the following kinetic scheme which applies at negative potentials during repolarization

$$C_3 \underset{\beta_3}{\leftarrow} C_4 \overset{\alpha_4}{\underset{\beta_4}{\rightleftarrows}} O$$

This scheme is in fact contained in the model presented in this paper (Table 2), and its salient feature is that, upon repolarization, the forward rate constant α_4 between the last closed and the open state is not zero giving a deactivation with two eigenvalues (see Goldman (1991)): one of them close to the value of β_4 and the other close to the value of β_3. The magnitude of the fast component of the tail increases as the value of α_4 decreases. It is clear that in the limiting case when α_4 is zero, the deactivation rate is a single exponential with rate β_4. The value of α_4 is not zero at the repolarization potential, because it has a very shallow voltage dependence, a requirement for the fit of the gating current and the prediction of the shallow voltage dependence of the open probability at positive potentials where the Q-V curve has essentially come to saturation. As most of the charge is in the step between C_3 and C_4 (valence of 3.5, see Table 2), the main time constant of the gating current tail is close to the value of $1/\beta_3$. In the model the fraction of the field in the return path of this transition is 0.19 giving a voltage dependence for β_3 that translates into an e-fold change every 37.6 mV. This value compares very well with the voltage dependence of the main decaying exponential of the gating current tail (Fig. 9 *b*) which changes by e-fold in about 35 mV at around -100 mV.

We thank Dr. D. E. Patton for reading and commenting on the manuscript. Supported by United States Public Health Services Grant GM30376 to F.B. and AR38970 to E.S. E.P. was supported by the Pew Charitable Trust.

REFERENCES

Armstrong, C. M., and F. Bezanilla. 1973. Currents related to movement of the gating particles of the sodium channel. *Nature (Lond.)*. 242:459–461.

Armstrong, C. M., and F. Bezanilla. 1977. Inactivation of the sodium channel. II. Gating current experiments. *J. Gen. Physiol.* 70:567–590.

Armstrong, C. M., and W. F. Gilly. 1979. Fast and slow steps in the activation of sodium channels. *J. Gen. Physiol.* 74:691–711.

Bezanilla, F., E. Perozo, D. M. Papazian, and E. Stefani. 1991. Molecular basis of gating charge immobilization in Shaker potassium channels. *Science (Wash. DC)*. 254:679–683.

Cole, K. C., and J. W. Moore. 1960. Potassium ion current in the squid giant axon: dynamic characteristic. *Biophys. J.* 1:1–14.

FitzHugh. R. 1965. A kinetic model of the conductance changes in nerve membrane. *J. Cell. Comp. Physiol.* 66:111–117.

Goldman, L. 1991. Gating current kinetics in *Myxicola* giant axons. Order of the back transition rate constants. *Biophys. J.* 59:574–589.

Hodgkin, A. L, and A. F. Huxley. 1952. A quantitative description of membrane current and its application to conduction and excitation in nerve. *J. Physiol. (Lond.)*. 117:500–544.

Hoshi, T., W., Zagotta, W. N., and Aldrich, R. W. 1990. Biophysical and Molecular Mechanisms of *Shaker* Potassium Channel Inactivation. *Science* 250:533–538.

MacKinnon R. 1991. Determination of the subunit stoichiometry of a voltage-activated potassium channel. *Nature (Lond.)*. 350:232–235.

Oxford, G. S. 1981. Some kinetic and steady-state properties of sodium channels after removal of inactivation. *J. Gen. Physiol.* 77:1–22.

Perozo, E., D. M. Papazian, E. Stefani, and F. Bezanilla. 1992. Gating currents in Shaker K^+ channels. Implications for activation and inactivation models. *Biophys. J.* 62:160–171.

Perozo, E., R. MacKinnon, F. Bezanilla, and E. Stefani. 1993. Gating currents from a non-conducting mutant reveal open-close conformations in *Shaker* K^+ channels. *Neuron*. 11:353–358.

Schoppa, N. E., K. McCormack, M. A. Tanouye, and F. J. Sigworth. 1992. The size of gating charge in wild-type and mutant *Shaker* potassium channels. *Science (Wash. DC)*. 255:1712–1715.

Sigg, D., E. Stefani, and F. Bezanilla. 1994. Gating current noise produced by elementary transitions in *Shaker* K^+ channels. *Science*. In press.

Spires, S., and T. Begenisich. 1989. Pharmacological and kinetic analysis of K channel gating currents. *J. Gen. Physiol.* 93:263–283.

Stefani, E., E. Perozo, L. Toro, and F. Bezanilla. 1994. Gating of Shaker K^+ channels: I. Ionic, and gating currents. *Biophys. J.* 66:996–1010.

Stühmer, W., F. Conti, M., Stocker, O. Pongs, and S. H. Heinemann. 1991. Gating currents of inactivating and non-inactivating potassium channels expressed in *Xenopus* oocytes. *Pfugers Arch.* 418:423–429.

Taglialatela, M., L. Toro, and E. Stefani. 1992. Novel voltage clamp to record small, fast currents from ion channels expressed in *Xenopus* oocytes. *Biophys. J.* 61:78–82.

Tytgat, J., and P. Hess. 1992. Evidence for cooperative interactions in potassium channel gating. *Nature (Lond.)*. 359:420–423.

Vandenberg, C. A., and F. Bezanilla. 1991. A model of sodium channel gating based on single channel, macroscopic ionic, and gating currents in the squid giant axon. *Biophys. J.* 60:1499–1510.

Zagotta, W. N., and R. W. Aldrich 1990. Voltage dependent gating of single Shaker A-type potassium channels in *Drosophila* muscle. *J. Gen. Physiol.* 95:29–60.

Zagotta, W. N, T. Hoshi, and R. W. Aldrich. 1990. Restoration of inactivation in mutants of Shaker potassium channels by a peptide derived from ShB. *Science (Wash. DC)*. 250:568–571.